



118  
480  
THS



This is to certify that the  
thesis entitled  
HIGH TEMPERATURE  $\text{Al}_2\text{O}_3$  DIFFUSION BARRIERS  
BY REACTIVE D.C. MAGNETRON SPUTTERING  
presented by

Zhiwei Cai

has been accepted towards fulfillment  
of the requirements for

~~MASTER~~ degree in ~~SCIENCE~~



Dr. D.S. Grummon

Major professor

Date ~~My/15~~ May 15th, 1992

# LIBRARY Michigan State University

PLACE IN RETURN BOX to remove this checkout from your record.  
TO AVOID FINES return on or before date due.

DATE DUE	DATE DUE	DATE DUE
SEP 25 1994	_____	_____
<del>SEP</del> 11 1994	_____	_____
_____	_____	_____
_____	_____	_____
_____	_____	_____
_____	_____	_____
_____	_____	_____

MSU is An Affirmative Action/Equal Opportunity Institution

c:\cir\datedue.pm3-p.1

HIGH TEMPERATURE  $\text{Al}_2\text{O}_3$  DIFFUSION BARRIERS  
BY REACTIVE D.C. MAGNETRON SPUTTERING

By  
Zhiwei Cai

A THESIS

Submitted to  
Michigan State University  
in partial fulfillment of the requirements  
for the degree of

MASTER OF SCIENCE

Department of Materials Science and Mechanics

1992



## ABSTRACT

This study has investigated aluminum oxide films, which were formed by reactive d.c. megnetron sputter deposition, to determine their effectiveness as diffusion barriers in two systems: monolithic TZ-Molybdenum (TZM), and a SiC particulate reinforced  $\text{Ni}_3\text{Al}+\text{B}$  composite. The film composition was  $\text{Al}_2\text{O}_x$ , where x was between 3.94 to 4.24.

In the study of the TZM system, two layers of  $2.42\text{ }\mu\text{m}$  thick as-deposited films were placed between two monolithic TZM plates. The films functioned as excellent diffusion barriers during hot compression at temperatures up to  $1500\text{ }^\circ\text{C}$ . However, oxidation occurred on the interfaces of TZM substrate owing to the excess oxygen in the film.

In the investigation of the SiC/ $\text{Ni}_3\text{Al}$  system, SiC particulates with a  $0.17\text{ }\mu\text{m}$  thick oxide film coatings were incorporated into an intermetallic matrix composite with  $\text{Ni}_3\text{Al}$ . The oxide film did not stop inter-diffusion between SiC and  $\text{Ni}_3\text{Al}$ . Ni diffused into SiC and formed compounds with both Si and Al. A Ni-Al-O compound was formed between the reaction zone and the matrix. Nevertheless, the film reduced the diffusion rates of elements in the system.

## ACKNOWLEDGMENT

I wish to express my sincere appreciation to Dr. D. S. Grummon, my advisor, for his generous support, patient guidance, creative ideas and scientific expertise. I would also like to thank my committee members, Dr. M. A. Crimp and Dr. T. R. Bieler, for their helpful discussions and valuable criticisms of the thesis. Also, the generosity of the Composite Materials and Structures Center for letting me use their equipment is appreciated.

## TABLE OF CONTENTS

LIST OF FIGURES	iv
LIST OF TABLES	vi
CHAPTER I. INTRODUCTION	1
CHAPTER II. LITERATURE REVIEW	5
1. Diffusion and Diffusion Bonding	5
1.1. Diffusion Across Interfaces	5
1.2. Diffusion Bonding	6
1.3. Behavior of TZ-Molybdenum Alloy at High Temperature	7
2. Interface Phenomena in High Temperature Metal Matrix Composites (MMCs) and Intermetallic Matrix Composites (IMCs)	8
2.1. Interface between Reinforcement and Matrix	8
2.2. SiC Reinforced High Temperature Composites	9
3. Diffusion Barrier	10
3.1. Candidates for Prevention of Diffusion Bonding	10
3.2. Al <sub>2</sub> O <sub>3</sub> as a Diffusion Barrier	11
4. Sputter Deposition	13

<b>CHAPTER III. SPUTTERED <math>\text{Al}_2\text{O}_3</math> DIFFUSION BARRIERS ON TZ-MOLYBDENUM ALLOY (TzM)</b>	<b>16</b>
1. Introduction	16
2. Experimental Procedures	16
2.1. $\text{Al}_2\text{O}_3$ Film Deposition and Examination	16
2.2. Characterization of Barrier Performance	20
3. Experimental Results and Discussion	22
3.1. As-deposited Film Examination	22
3.2. As-deposited Oxide Film as a Diffusion Barrier for TZ-Molybdenum Alloy	30
4. Summary	32
 <b>CHAPTER IV. AN <math>\text{Al}_2\text{O}_3</math> DIFFUSION BARRIER FOR A SiC/<math>\text{Ni}_3\text{Al}+\text{B}</math> COMPOSITE</b>	 <b>36</b>
1. Introduction	36
2. Experimental Procedures	38
2.1. $\text{Al}_2\text{O}_3$ Film Deposition and Examination	38
2.2. Diffusion Bonding of SiC/ $\text{Ni}_3\text{Al}+\text{B}$ Composite	38
3. Experimental Results and Discussion	40
3.1. Film Deposition and Examination	40
3.2. As-deposited Oxide Film as a Diffusion Barrier for SiC/ $\text{Ni}_3\text{Al}+\text{B}$ Composite	44
4. Summary	49

<b>CHAPTER V. CONCLUSIONS</b>	<b>51</b>
-------------------------------	-----------

<b>BIBLIOGRAPHY</b>	<b>54</b>
---------------------	-----------

## LIST OF FIGURES

Figure 1.	D.C. Magnetron Sputtering Apparatus	17
Figure 2.	Mask and the Film Coating with the Mask Applied	18
Figure 3.	Configuration of TZM Hot Pressing Test	21
Figure 4.	Surface Survey for As-deposited Film and C Peak Fitting, before Sputtering, by XPS	24
Figure 5.	Carbon Peak Fitting, before Sputtering	24
Figure 6.	Al Peak of As-deposited Film after 8 min. Sputtering, by XPS	25
Figure 7.	O Peak of As-deposited Film after 8 min. Sputtering, by XPS	25
Figure 8.	AES Profiling of Sample with 0.087 $\mu\text{m}$ Thick Film	28
Figure 9.	AES Profiling of Sample with 0.34 $\mu\text{m}$ Thick Film	28
Figure 10.	Image of Cross-Section of the As-deposited Oxide Film, by SEM	29
Figure 11.	Surface Morphology of the As-deposited Oxide Film on TZM Substrate, by SEM	29
Figure 12.	Sketch of the Interface of the Hot Pressed TZM Plates, after Separation	30
Figure 13.	Interface of TZM Plate, after Hot-Pressing at 1200 $^{\circ}\text{C}$ , by SEM	33
Figure 14.	Interface of TZM Plate, after Hot-Pressing at 1500 $^{\circ}\text{C}$ , by SEM	33
Figure 15.	Region A of Figure 14, Surface Element Information, by EDX	34
Figure 16.	Region B of Figure 14, Surface Element Information, by EDX	34
Figure 17.	Line Scanning for Al, O, Mo, on the 1300 $^{\circ}\text{C}$ TZM Specimen, by AES	35
Figure 18.	SEM Image of Line Scanning on the 1300 $^{\circ}\text{C}$ TZM Specimen, by AES	35

Figure 19. Configuration of SiC Particulates/Ni <sub>3</sub> Al Diffusion Bonding Couple	39
Figure 20. AES Profiling of Film on SiC Particulate	42
Figure 21. As-deposited Film on the Edge of a SiC Particulate Substrate, by SEM	43
Figure 22. Optical Micrograph for Sample of 1000 °C, 500×: (a) As-polished; (b) Etched	46
Figure 23. Optical Micrograph for the Specimen of 1100 °C/12 hours, 50×	47
Figure 24. Line Scanning for Ni, Al, O, Si on Sample of 1100 °C/3 hours, by AES	50
Figure 25. SEM Image of Line Scanning on Sample of 1100 °C/3 hours, by AES	50

## LIST OF TABLES

Table 1. Summary of Film Thicknesses	22
Table 2. Results from Curve Fitting for C Peak, before Sputtering, by XPS	24
Table 3. Results from Curve Fitting for Al and O Peaks, after 8 Minutes Sputtering, by XPS	25
Table 4. Elemental Concentrations in As-deposited Film, by XPS	26



## CHAPTER I. INTRODUCTION

This project was motivated by a real problem existing in a high-temperature material properties testing system, in this case an MTS-810 high temperature fatigue testing system. Combining a servo hydraulic loading system and a vacuum furnace, this system has a capability to test materials at temperatures up to 1700 °C. However, it has a potential problem: The diffusion bonding among the loading fixtures may cause them to bond at temperature over 1100 °C. In the system, TZ-Molybdenum alloy (TZM) is used for the loading fixtures. Thus, a suitable diffusion barrier for this alloy was needed to prevent the diffusion bonding among the fixtures at such high temperature.

Another related, but separate, problem also motivated this project. In metal and intermetallic matrix composites for high temperature applications, severe diffusion and/or reaction between reinforcements and matrices may occur due to high concentration gradients across the interface. In most cases, inter-diffusion and diffusion-controlled reactions degrade the reinforcements, and may be detrimental to composite mechanical properties. This is the case in SiC reinforced nickel and nickel aluminide matrix composites. A diffusion/reaction barrier is needed between the reinforcement and matrix in these cases. It has been shown

by Nieh [1988]<sup>1</sup> that a 0.13  $\mu\text{m}$  thick  $\text{Al}_2\text{O}_3$  film formed by preoxidizing a nickel aluminide alloy (IC-50) can prevent inter-diffusion between planar SiC and nickel aluminide. The second part of the project, then, has been to investigate the effectiveness of a reactive d.c. sputter-deposited aluminum oxide film of 0.17  $\mu\text{m}$  thickness which acts as a diffusion barrier in a SiC particulate reinforced  $\text{Ni}_3\text{Al}+\text{B}$  composite.

As a mass transport process, diffusion behavior is directly related to the mobility and the gradient of the chemical potential of atoms. The chemical potential of an element is, in many cases, proportional to its atomic concentration. Therefore, the gradient of atomic concentration of element is usually the driving force of diffusion.

An example of diffusion driven by gradient of atomic concentration is diffusion in a binary-element couple. The inter-diffusion among elements may be inevitable at high temperature because of the sharp concentration gradient across the interface. The Kirkendall phenomenon, which is the phenomenon that the original interface (or the marks on the original interface) migrates in response to the net diffusing flux, is usually observed in such cases because of different diffusion rates among the diffusion species.

---

<sup>1</sup> The citation in this paper is listed according to the last name of the first author of the references.

In some practical situations, such as in high temperature testing system, the diffusion between the specimen and the grip components will cause them to become diffusion bonded, which is not desirable. Diffusion barriers are necessary to prevent the unwanted diffusion in such situations.

Candidates for effective diffusion barrier are often stable compounds. They include the transition metal carbides (HfC, TaC, TiC), nitrides (HfN, TiN), borides (TiB<sub>2</sub>), and oxides (Al<sub>2</sub>O<sub>3</sub>, HfO<sub>2</sub>, Y<sub>2</sub>O<sub>3</sub>, etc.).

Al<sub>2</sub>O<sub>3</sub> has long been considered an attractive candidate for high temperature diffusion barriers, because of its high melting point, high chemical stability at very high temperature, low solubility, and relatively high thermal expansion coefficient. Thus, it is reasonable to choose Al<sub>2</sub>O<sub>3</sub> film as the diffusion barrier for the TZM in this study.

A reactive d.c. sputter deposition method is attractive for depositing Al<sub>2</sub>O<sub>3</sub> film because the d.c. sputter deposition method is simple, power-effective, and has a modest effect on the properties of the substrate. With oxygen added to the sputtering atmosphere, a d.c. sputtered pure aluminum target can produce an aluminum oxide film on the substrate.

In this study, aluminum oxide films deposited onto various substrates by reactive d.c. sputtering method were applied as diffusion barriers for both TZM components in a

Mechanical High Temperature Test System, and for a SiC particulate reinforced  $\text{Ni}_3\text{Al}+\text{B}$  composite. A special levitation device was made to deposit the oxide films onto SiC particulates. A hot-pressing test was used for studying the effectiveness of such diffusion barriers at various temperatures. To examine the as-deposited films and to characterize the barriers' performance, several methods were applied, including optical microscopy, scanning electron microscopy (SEM), energy dispersive X-ray emission spectroscopy (EDX), Auger electron spectroscopy (AES), and X-ray photoelectron spectroscopy (XPS).

The following chapter presents a review of previous work in the related fields of diffusion, interfacial phenomena, diffusion barriers, and sputter deposition processes. It will be followed by discussion of experimental methods, results, and conclusions drawn from the study.

## CHAPTER II. LITERATURE REVIEW

### 1. Diffusion and Diffusion Bonding

#### 1.1. Diffusion Across Interfaces

Diffusion underlies many changes in material structure which lead to alteration of the physical and mechanical properties of materials. As a mass transport process, the diffusion flux of a element in the material is a function of the gradient of its atomic concentration ( $x_i$ ):

$$J_i = -D_i \nabla(x_i)$$

where,  $J_i$  is the flux of element  $i$ ;  $D_i$  is the diffusivity of this element in material; and  $\nabla$  means the gradient.

In a diffusion couple, the concentration gradients across the interface are sharp. Thus, in many cases, interdiffusion is inevitable at elevated temperature. For instance, a Ni-Cu couple will undergo a substitutional diffusion at elevated temperature. Since the diffusivities of different elements are different, substitutional solutes do not generally diffuse into each other at equal and opposite rates. A net transport of atoms flows from the side with higher diffusivity to the other side with lower diffusivity, leaving more than the equilibrium concentration of vacancies behind. Therefore, the original interface (or

the marks on the original interface) will migrate to the opposite direction in response to this net flux. The extra vacancies can coalesce to form voids. This phenomenon is known as the Kirkendall Effect [Shewmon, 1963; Verhoeven, 1975].

However, in some cases diffusion of one element may not be observed even though there is a gradient of concentration. In such cases, a low diffusivity of this element is necessary in order to have a negligible diffusion flux. Usually, metal elements have low diffusivities in stable compounds. For instance, Ni has a low diffusivity in many oxides, such as MgO, CaO, and amorphous SiO<sub>2</sub> [Nieh, 1988].

## 1.2. Diffusion Bonding

One useful application of diffusion phenomena is *diffusion bonding*. It is a well-known technique for solid-state joining in which two surfaces are joined at an elevated temperature using an applied interfacial pressure. Diffusion among elements eliminates the interface between two solids. This method has been applied to fabricate metal- and intermetallic- matrix composites [Kreider, 1974; Schoutens, 1982].

Diffusion bonding requires a combined effect of temperature, pressure and processing time. It has a threshold value of temperature-pressure-time parameter to

ensure bonding and elimination of interfacial voids. In this parameter, temperature is the most important factor. Usually the bonding temperature is above the materials' recrystallization temperatures, which is in the range of 0.5 - 0.9  $T_m$  (where  $T_m$  is the absolute melting point of the bonding material). The required processing time is affected mostly by the bonding temperature, which decreases with increasing temperature. A sufficient interfacial pressure must be applied in order to have good contact between bonding components. Though higher pressure enhances the bonding, its influence is minor comparing to the effects of temperature and processing time. Furthermore, any roughness of the interfaces reduces the effectiveness of contact of bonding components under the pressure.

### 1.3. Behavior of TZ-Molybdenum Alloy at High Temperature

TZ-Molybdenum (TZM) is a low carbon content molybdenum alloy with Ti and Zr alloying additives (Mo-0.5% Ti-0.1% Zr-0.01% C), which was originally developed as a stronger high-temperature material needed for aerospace applications. It has a similar melting point to Mo, at about 2600 °C, but has a tensile strength approximately twice that of Mo above 1093 °C [Savitskii, 1970; Walters, 1988]. The recrystallization temperature of TZM is about 1100 °C (1373 K). Thus, diffusion bonding between TZM components is possible if the application temperature is higher than this temperature. Therefore, a

diffusion barrier may be necessary for TZM components when the service temperature is higher than 1100 °C, especially for applications under conditions of large loading and long period of time.

## 2. Interface Phenomena in High Temperature Metal Matrix Composites (MMCs) and Intermetallic Matrix Composites (IMCs)

### 2.1. Interface between Reinforcement and Matrix

Many ceramic fiber-reinforced metal matrix composites (MMCs) and intermetallic matrix composites (IMCs) are of interest for elevated-temperature applications [Brindley, 1987; Metcalfe, 1974; Schoutens, 1982].  $\text{Al}_2\text{O}_3$  and SiC fiber reinforced Ni-based alloys and nickel aluminide based alloys are among the most interesting composites for high-temperature applications because they promise theoretically good properties at temperatures over 1000 °C [Mehan, 1974; Pope, 1986; Yang (1), 1989]. However, many composite systems suffer an inter-diffusion and/or interfacial reactions between the matrix and reinforcement during processing and application at high temperature.

In composites, the non-equilibrium state at the interface between the reinforcement and matrix is caused by a sharp gradient in chemical potential that becomes the driving force for diffusion. This is especially realized during high



temperature processing or the intended high temperature application for high temperature composites [Chou, 1985; Reddy, 1989].

Inter-diffusion and/or interfacial reactions often degrade the reinforcement. The reaction products in the interfacial region are usually brittle. This is detrimental to the composite strength. Therefore, a mechanical bond between the reinforcement and matrix is preferred, especially for high temperature composites [Schoutens, 1982], although a limited degree of inter-diffusion between reinforcement and matrix may establish a good bonding [Broutman, 1974].

## 2.2. SiC Reinforced High Temperature Composites

SiC reinforced Ni-based MMCs and Ni<sub>3</sub>Al-based IMCs are typical examples of high temperature composites currently of interest. Because of the severe reaction between SiC and these matrices, SiC reinforcement of Ni- and Ni<sub>3</sub>Al- based alloys is still difficult because of the tendency toward degradation of the SiC reinforcement.

SiC reacts with Ni and Ni-based alloys in both vacuum and air environments between 700 and 1150 °C [Jackson, 1983]. The kinetic rate of the reaction is diffusion controlled. Ni is the predominant species diffusing into SiC, although other alloying elements also diffuse into SiC [Jackson, 1983; Mehan, 1979].

The diffusion of Ni into SiC forms a banded structure consisting of alternating layers of  $\delta$ -Ni<sub>2</sub>Si and a two-phase mixture of graphite and  $\delta$ -Ni<sub>2</sub>Si. On the matrix side, both the reaction products and the reaction degree is very dependent upon the presence of alloying elements. The reaction of a pure Ni matrix has the most severe, followed by NiCr and NiCrAl matrices [Jackson, 1983]. For NiCrAl matrix, the product at the matrix side is a mixture of four phases:  $\gamma'$ -Ni<sub>3</sub>Al,  $\beta$ -NiAl,  $\alpha$ -Cr and a ternary Ni-Si-Al phase [Hall, 1983]. Cracks are found in the reaction zone.

There is also a reaction between SiC fiber and Ni<sub>3</sub>Al-based alloys at temperatures above approximately 1073 K. It is similar to the reaction between SiC and Ni-based alloys, but with about five times slower reaction rate. Ni is the dominant diffusing species controlling the overall reaction rate [Nieh, 1988; Yang (2) and Yang (3), 1989].

Therefore, using diffusion barriers between SiC and these matrices is inevitable for the composites elevated temperature services.

### 3. Diffusion Barriers

#### 3.1. Candidates for Prevention of Diffusion Bonding

Many high temperature alloy coatings (Ni-, Fe-, Co-based alloys with Cr, Ti, Al, V additives) are used as

barriers for prevention of diffusion bonding. The protection mechanism of those coatings is based on adherent impervious surface films of  $\text{Al}_2\text{O}_3$ ,  $\text{SiO}_2$ ,  $\text{CrO}_3$ , or a spinel-type that grows on high temperature exposure to air [Grayson, 1983].

Therefore, a direct way of preventing diffusion bonding would be using any of the oxides as a diffusion barrier, although the thermal expansion coefficient mismatch of the oxide coating and the substrate can cause stress during thermal cycling. Other kinds of stable compounds, including the transition metal carbides ( $\text{HfC}$ ,  $\text{TaC}$ ,  $\text{TiC}$ ), nitrides ( $\text{TiN}$ ,  $\text{HfN}$ ) and borides ( $\text{TiB}_2$ ), can also be used as diffusion barriers in various situations [Walters, 1988].

### 3.2. $\text{Al}_2\text{O}_3$ as a Diffusion Barrier

$\text{Al}_2\text{O}_3$  is an excellent general candidate for diffusion barriers. It has high melting point (2072 °C or 2345 K), moderate thermal shock resistance, good stability at high temperature in a wide variety of atmospheres, and is a good electric insulator at high temperature. A reasonably good and nearly constant strength can be maintained at temperatures up to about 1000 - 1100 °C.

$\text{Al}_2\text{O}_3$  has a relatively high thermal expansion coefficient ( $8 \times 10^{-6}/^\circ\text{C}$ ), compared to other ceramics like  $\text{SiC}$  ( $4.7 \times 10^{-6}/^\circ\text{C}$ ). This value fits in between  $\text{SiC}$  and  $\text{Ni}$  or  $\text{Ni}_3\text{Al}$  ( $12 \times 10^{-6}/^\circ\text{C}$ ), which can limit the internal stress due to the

thermal cycling if an  $\text{Al}_2\text{O}_3$  film is coated onto SiC reinforcement in SiC reinforced Ni- or  $\text{Ni}_3\text{Al}$ -based matrix composites [Grayson, 1983; Nourbakhsh, 1989].

Furthermore, oxides are the most effective barriers for Ni diffusion because Ni has low diffusion coefficients in oxides. For instance, Ni has a diffusivity in a range of  $10^{-13}$  to  $10^{-12}$   $\text{m}^2/\text{s}$  in amorphous  $\text{SiO}_2$  over a temperature range of 1000 to 1200 °C [Goshtagore, 1969]. Nieh [1988] has demonstrated that  $\text{Al}_2\text{O}_3$  film on SiC fiber can be applied successfully as a diffusion barrier between planar SiC and  $\text{Ni}_3\text{Al}$ -based alloy.

In Nieh's experiment, the nickel aluminide was IC-50 (Ni-23 at% Al-0.5 at% Hf-0.2 at% B) which was preoxidized to form an  $\text{Al}_2\text{O}_3$  surface film. The preoxidation was performed at 1000 °C in air for 60 hours, after which a 0.13  $\mu\text{m}$  thick  $\text{Al}_2\text{O}_3$  layer was formed. Subsequent diffusion bonding was carried out using the preoxidized aluminide plate and a SiC disc. There was no bond even at 1100 °C, suggesting that  $\text{Al}_2\text{O}_3$  is a good diffusion barrier for high temperature SiC/aluminide reaction.

However, the preoxidation method has its limitation. It can only be used for a few materials which contain certain oxidation reactive elements, such as Al, Cr. Furthermore, this method may alter the composition of the material, especially near the surface region. On the other hand, other

method such as *sputter deposition* has many advantages for thin film formation over the preoxidation method.

#### 4. Sputter Deposition

Sputter deposition is a process under vacuum in which atoms of the cathode (target) material is ejected by the bombardment of positive ions and energetic particles in an electrical discharge, and then condensed onto a substrate [Holland, 1974]. Sputter deposition offers many advantages including its reliable reproducibility, continuous nature, and simplicity. Sputtering is a complex process, and has been extensively studied [Behrisch, 1981 and 1983].

Under bombardment by energetic positive ions and other particles, the atoms on the target undergo a momentum exchange process with bombarding particles. After obtaining sufficient momentum, the target atoms leave the target with a relatively high kinetic energy (in an average of 5 - 30 eV) [Westwood, 1988]. Because the momentum exchange process is influenced by the relative atom mass and bonding energy with other target atoms, the sputtering yield (the number of yield atoms per incident particle) is different from element to element. Thus, the composition of an alloy target surface will change at the beginning of sputtering. This phenomenon is called *preferential sputtering*. However, the sputtering yield is also affected by the atom's concentration on the

target surface. Therefore, after a certain period of time, the composition of target surface will become steady, provided the target is cold enough to prohibit the diffusion within the target. The sputtered flux is then constrained to match the bulk target alloy composition.

Sputter deposition can deposit films that are very thin (1 - 50,000 Å), and fully dense. The deposited film can have a high degree of adherence to the substrate surface [Mattox, 1989]. Also it has been shown that for film deposited onto fibers, d.c. sputter coating processes have little effect on substrate strength [Brown, 1986; Mehan, 1974].

Reactive sputtering refers to a sputter deposition technique in which reactive gas is added to the deposition atmosphere to react with the growing film to form a compound. Reactive d.c. sputter deposition is one of the reactive sputtering methods. It uses a metallic target to produce the desired compound, like oxide or nitride, with a reactive gas flow [Holland, 1974; Mattox, 1989]. Using pure Al to form an aluminum oxide layer is one example [Pang, 1989].

During deposition, the oxygen admitted into the chamber is to form an oxide with the sputtered Al. However, it can also react with the "fresh" sputtered Al target. If the whole surface of the target becomes oxide because of a high oxygen flow admitting into the chamber, a stable plasma will not be maintained under a d.c. condition owing to the insulating of the target surface. This is called the target

*poisoning*. Therefore, the oxygen flow has to be controlled under a certain level for a stable plasma in a reactive d.c. sputtering process.

# CHAPTER III. SPUTTERED $\text{Al}_2\text{O}_3$ DIFFUSION BARRIERS ON TZ-MOLYBDENUM ALLOY (TZM)

## 1. Introduction

The main objective of this study is to investigate the effectiveness of  $\text{Al}_2\text{O}_3$  films as diffusion barrier for TZ-Molybdenum alloy (TZM). The films were coated by reactive d.c. sputtering method onto planar TZM substrates and then hot-pressed between two TZM plates. The performance of films with respect to their ability to prevent diffusion bonding of the plates was examined after the hot-pressing test.

## 2. Experimental Procedures

### 2.1. $\text{Al}_2\text{O}_3$ Film Deposition and Examination

A magnetron enhanced d.c. sputtering apparatus was used for film deposition in this study. The setup is shown schematically in Figure 1. With a turbomolecular pump (Model CFF 450, from Alcatel Inc.), it was possible to have a base pressure as low as  $1 \times 10^{-7}$  torr. The working gas (argon) was monitored and controlled by a 2-gas electron impact spectrometer-type partial pressure controller (Model OGCl, from INFICON Company). The target was a commercially pure aluminum alloy (1100 alloy) ( $\text{Al}+1 \text{ wt\% (Si+Fe)}$ ).



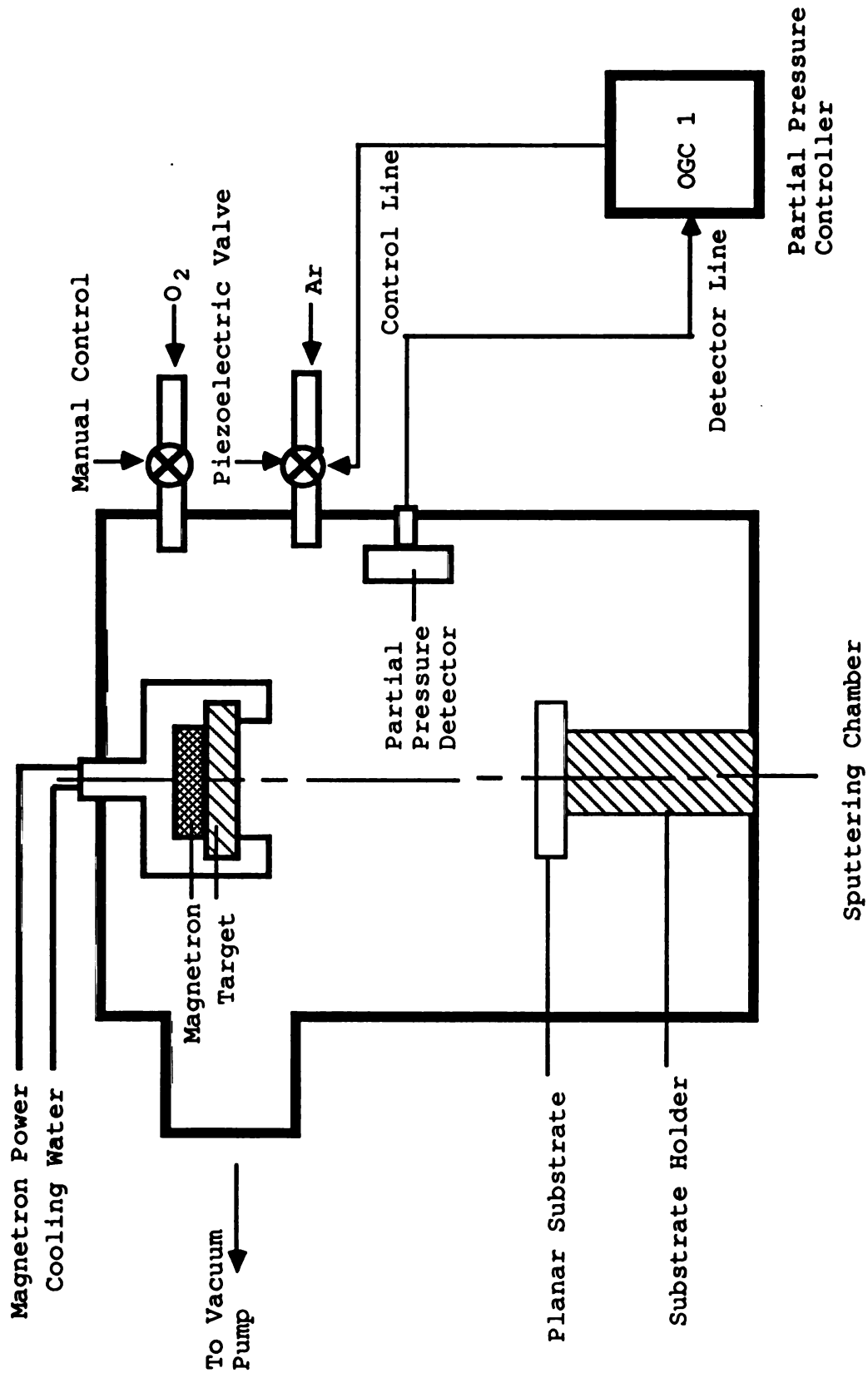
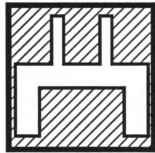
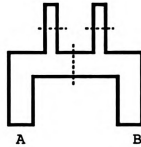


Figure 1. D.C. Magnetron Sputtering Apparatus



(a) . Mask



(b) . Film by the Mask

Figure 2. Mask and the Film Coating with the Mask Applied

In this study, three kind of substrates were used, including glass, TZM, and brass plates. In all runs, a glass substrate with a mask was included for use in film thickness and electric resistance measurements. The mask was made of stainless steel sheet and had a window with four legs, which is usually used for preparing films for four-point resistivity measurement. Figure 2(a) shows the sketch of the mask and Figure 2(b) illustrates the film coated on a planar glass substrate with the mask. In this study, however, the resistance was simply measured across two legs labeled 'A' and 'B' in Figure 2(b) by a resistance meter. Such measurement provided a quick and easy way to determine if the as-deposited film was an insulator or not. The other two legs were used for film thickness measurement. Three dashed

lines in Figure 2(b) show the places for film thickness measurement.

In the film coating experiment, the parameters were: (1) Magnetron cathode input power: 300 W; (2) Working gas: Ar, at a partial pressure of  $5 \times 10^{-3}$  torr; (3) Target-substrates distance: 25 cm. The oxygen flow was controlled manually by a micrometer valve during the sputtering process.

In this study, it was found that a maximum oxygen flow allowing a stable plasma was corresponding to such a flow that would cause an oxygen partial pressure at about  $1 \times 10^{-3}$  torr if there were no plasma generated in the chamber. This maximum flow was maintained during all the reactive d.c. sputter deposition experiments.

After the as-deposited films were taken out from the vacuum chamber, an electric resistance measurement was made to determine whether the as-deposited films were insulating or conductive. The composition of the films on TZM substrates was determined by X-ray photoelectron spectroscopy (XPS) (PHI 54000, Perkin-Elmer). The as-deposited films on two brass plates were used for elemental depth-profiling examination by Auger electron spectroscopy (AES) (PHI 660, Perkin-Elmer).

The film thickness measurement was done with a DEKTAK-II profilometer on the masked glass substrate specimen. An average value of the measurements at three different places

on each film, the dashed lines shown in Figure 2(b), was used as the film thickness. After that, scanning electron microscopy (SEM) (Hitachi S-2500C) was used to examine coating quality of the as-deposited films. The film on a glass substrate was fractured, and the cross-section was observed. The film on the TZM substrate was used for surface morphology observation by SEM.

## 2.2. Characterization of Barrier Performance

A TZM plate with the as-deposited oxide film was cut into small slices. Each two of these slices were then placed as a couple in a way shown in Figure 3. The films on the two TZM slices were placed in contact. These couples were hot-pressed on MTS-810 high-temperature material test system in three different experimental conditions: 1200°C/100MPa/6 hours; 1300°C/100MPa/6 hours; and 1500°C/10MPa/6 hours. All the hot-pressing tests were performed in vacuum at pressures of  $10^{-5}$  to  $10^{-6}$  torr. The couple was separated from the MTS-810 fixtures by two  $\text{Al}_2\text{O}_3$  plates. After the hot-pressing tests, SEM, energy dispersive X-ray emission spectroscopy (EDX), and AES were used for interface examination for all un-bonded samples.

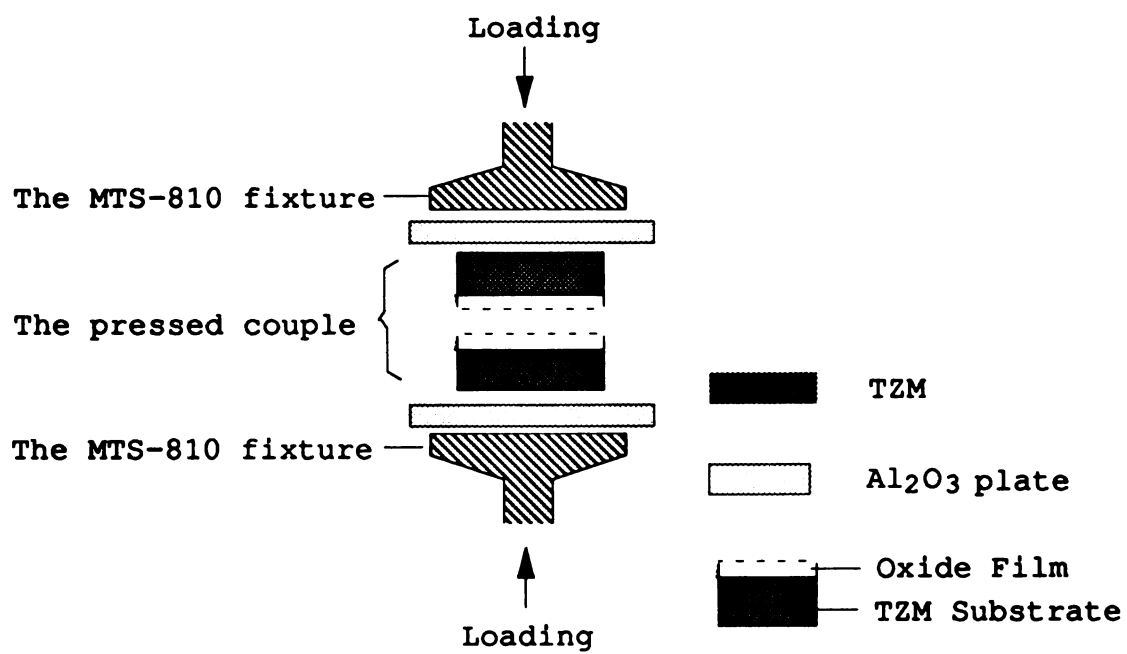


Figure 3: Configuration of TZM Hot Pressing Test

### 3. Results and Discussion

#### 3.1. As-deposited Film Examination

The thicknesses of all as-deposited films were measured and listed in Table 1. This measurement is essential for all following studies. Two films on brass substrates were used for calibrating the sputtering rate of AES profiling and for studying elemental depth-profiling of the films. The calibration was important because it would be used later for film thickness measurement on particulate substrate. The film on the TZM substrate was used as a diffusion barrier for TZM at high temperature. Thus, the film thickness was one of the important parameters of characterization of the barrier performance. In the table, the average value of three measurements is used as the thickness, and the upper and lower limits are also shown.

Table 1. Summary of Film Thicknesses

#	Substrate	Thickness	Comment
1	Glass	$1.38^{+0.01}_{-0.00} \mu\text{m}$	For SEM Cross-Section Observation
2	TZM	$2.42^{+0.06}_{-0.11} \mu\text{m}$	For Hot Pressing Test
3	Brass	$0.087^{+0.002}_{-0.001} \mu\text{m}$	For AES Profiling
4	Brass	$0.34^{+0.02}_{-0.04} \mu\text{m}$	For AES Profiling

Under the deposition condition, the oxygen partial pressure was lower than  $1 \times 10^{-6}$  torr (the lower limit of the partial pressure detector). It was significantly lower than it would be in the case without plasma. While in the case without plasma, the oxygen flow used in the experiments would cause a partial pressure of  $1 \times 10^{-3}$  torr. Therefore, aluminum oxide was expected in the as-deposited films. The as-deposited films were first examined by the electric resistance measurement. It was found that the films were insulators. The resistances of films were higher than the upper limit of the resistance meter ( $>30 \text{ M}\Omega$ ).

The composition of the as-deposited film was then studied by XPS. The surface surveys by XPS is shown in Figure 4. A carbon peak was found. It is from surface contamination of the sample. By using the curve fitting method, it was found that 36.28% of the carbon peak was contributed by two  $\text{CO}_x$  type bonds ( $x$  were close to 1 and 2, respectively), as seen in Figure 5. Table 2 is a summary of these results. After 8 minutes sputtering for surface contamination removal, only Al and O peaks were found. Most of the Al-O bond in the film was  $\text{Al}_2\text{O}_3$  (sapphire) type according to the curve fitting results, and the O-to-Al ratio was then 1.97. Figure 6 and 7 show the curve fits for the Al and O peaks after sputtering respectively, and the results are summarized in Table 3. The O-to-Al ratios in the film before and after sputtering cleaning are calculated and listed in Table 4.

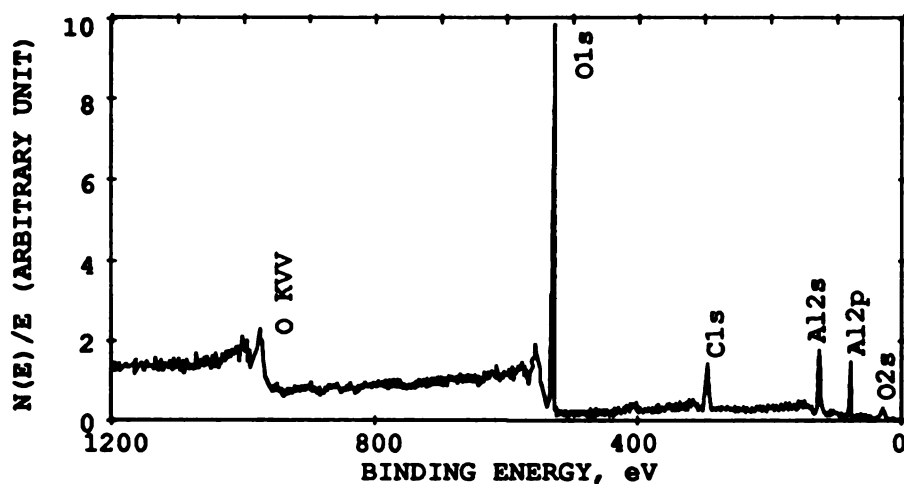


Figure 4. Surface Survey for the As-deposited Film, before Sputtering, by XPS

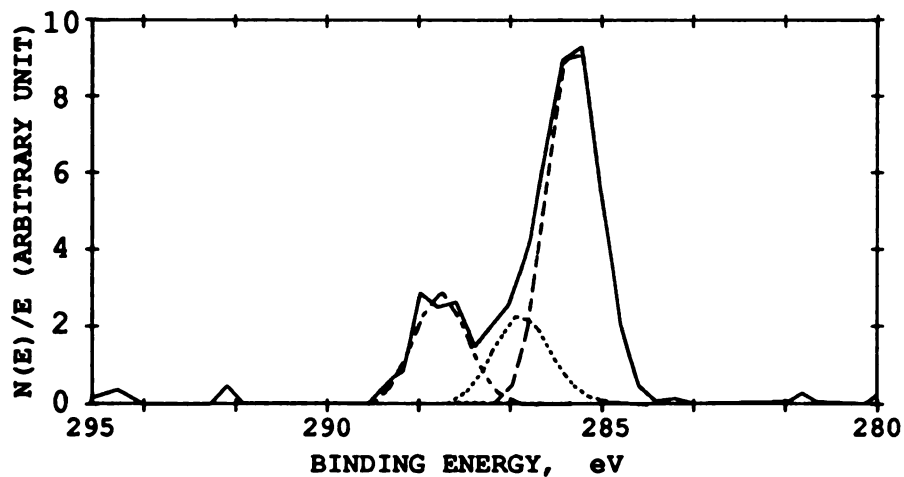


Figure 5. Carbon Peak Fitting, before Sputtering

Table 2. Results from Curve Fitting for C Peak, before Sputtering, by XPS.

Band No.	Position (eV.)	% of Total Area	Bond Type
1	285.74	63.72	C-C
2	287.31	16.63	CO <sub>x</sub> , x=1
3	289.54	19.66	CO <sub>x</sub> , x=2



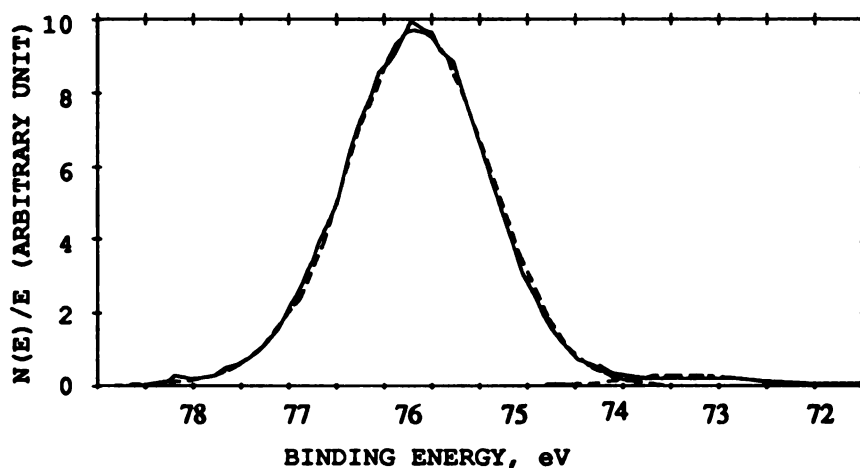


Figure 6. Al Peak of As-deposited Film,  
after 8 min. Sputtering, by XP

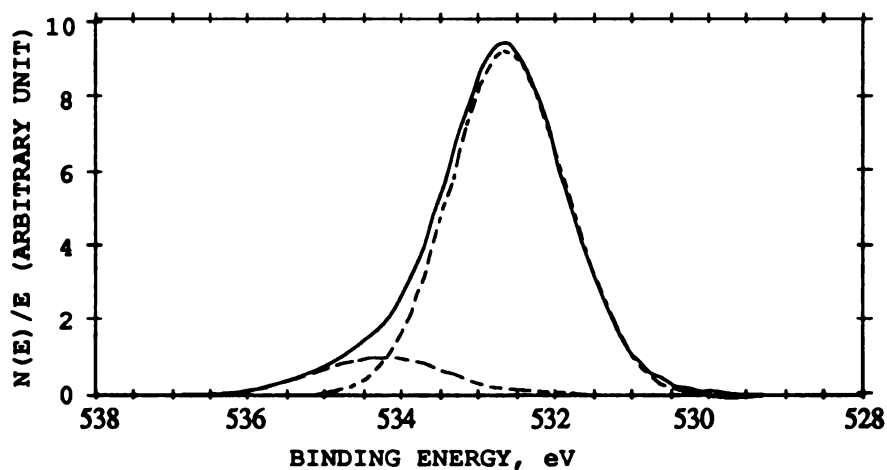


Figure 7. O Peak of As-deposited Film  
after 8 min. Sputtering, by XPS

Table 3. Results from Curve Fittings for Al and O Peaks,  
after 8 Minutes Sputtering, by XPS.

Element	Band No.	Position (eV.)	% of Total Area	Bond Type
Al	1	75.67	97.81	Al <sub>2</sub> O <sub>3</sub> , Sapphire
	2	72.82	2.19	
O	1	534.24	10.68	
	2	532.56	89.39	Al <sub>2</sub> O <sub>3</sub> , Sapphire

Table 4. Elemental Concentrations in As-deposited Film,  
by XPS.

	Before Sputtering	After 8 min. Sputtering
C (total)	21.93 at%	0 at%
C (from CO <sub>x</sub> )	7.96 at%	0 at%
O (total)	57.67 at%	66.28 at%
O (from the film)	45.4 at%	66.28 at%
Al	21.40 at%	33.72 at%
O-to-Al (in the film)	2.12 (Al <sub>2</sub> O <sub>4.24</sub> )	1.97 (Al <sub>2</sub> O <sub>3.94</sub> )

According to the XPS results, the O-to-Al ratio on the as-deposited film surface was in a range of 1.97 to 2.12, as shown in Table 4. In other words, the oxygen content in excess of the stoichiometry (Al<sub>2</sub>O<sub>3</sub>) in the as-deposited film was between 29.2% and 23.9%. The difference between the O-to-Al ratios before and after the surface contamination removal is caused by the preferential sputtering of oxygen, which is normally observed in oxide sputtering processes [Behrish, 1983].

The elemental depth-profiling information through the as-deposited films was investigated by AES profiling method. The films on two brass substrates were used. The profiling results showed that the concentrations of Al and O were consistent through the as-deposited films, indicating that the films were uniform in composition. The profiling results

are shown in Figure 8 and Figure 9 for the films of 0.087  $\mu\text{m}$  and 0.34  $\mu\text{m}$  thick respectively. The average profiling rate was 0.011  $\mu\text{m}/\text{minute}$  for the as-deposited films.

However, the information of element concentrations did not correspond precisely with the results from XPS. This is because the AES analysis is not good for chemical bond determination, but rather only shows qualitatively the existence of certain elements on sample's surface. The quantitative analysis of element concentration in AES is complicated and requires a series of calibrations. In this study, the combination of the XPS surface composition determination and the qualitative AES depth-profiling provides an efficient way to determine the composition and its distribution through the films.

Therefore, aluminum oxide films have been deposited by reactive d.c. sputtering method. With the oxygen flow used, the oxygen content in the film was in excess of the stoichiometry. A smaller flow then is necessary to form an aluminum oxide film with a stoichiometric composition.

Both cross-section and surface morphology of the films were observed in SEM for coating quality examination. The cross-section of the film showed that the film was fully dense and no evidence of grain boundary appeared on the cross-section under 15,000 $\times$  magnification, as seen in Figure 10. The surface morphology of the film on the TZM substrate, as seen in Figure 11, also showed a dense film. The pictured

area on Figure 11 was near the edge of the observed sample, and the substrate was only seen at the sample's edge area during the SEM observation. No evidences of grain boundary and crack were seen in the films.

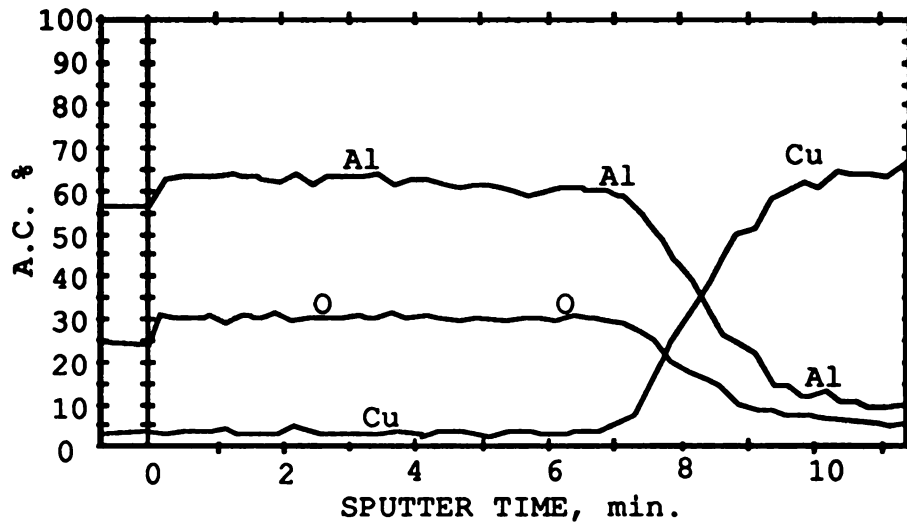


Figure 8. AES Profiling of Sample with 0.087  $\mu\text{m}$  Thick Film.

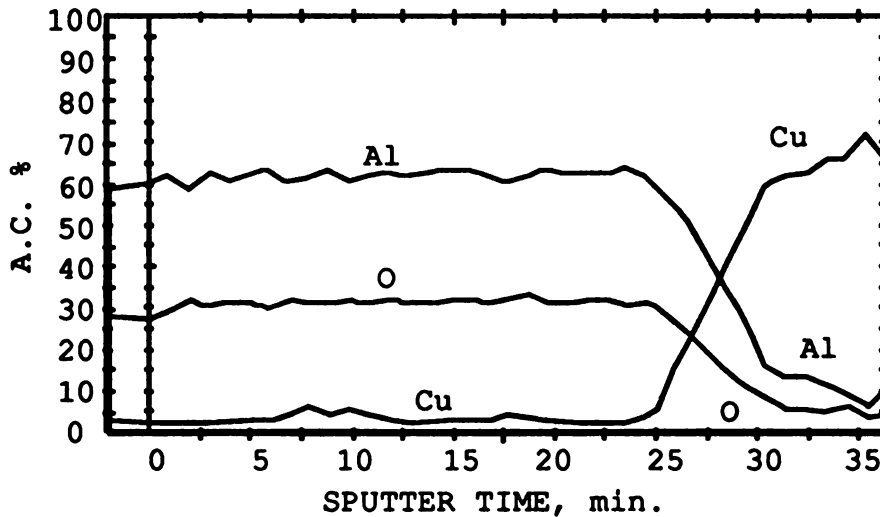


Figure 9. AES Profiling of Sample with 0.34  $\mu\text{m}$  Thick Film.



Figure 11. Surface Morphology of the As-deposited Oxide Film on TZO substrate, by SEM



Figure 10. Image of Cross-section of the As-deposited Oxide Film, by SEM

### 3.2. As-deposited Oxide Film as a Diffusion Barrier for TZ-Molybdenum Alloy

In order to assess the as-deposited aluminum oxide films effectiveness as diffusion barriers, two of the TZM plates with a layer of 2.42  $\mu\text{m}$  thick film were used in hot-pressing tests. No bonding between the hot-pressed couple was achieved under all three test conditions. After the separation of plates, the film tended to remain on one plate (plate A) in some areas while in other areas the film adhered to the other plate (plate B), leaving a bare TZM substrate on the opposite face. This is shown in the sketching in Figure 12. This suggested that the diffusion bonding between two aluminum oxide films was stronger than the bonding between the film and the TZM substrate.

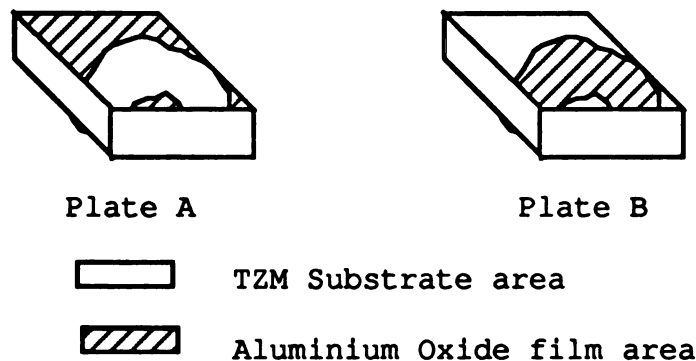


Figure 12. Sketch of the Interface of the Hot Pressed TZM Plates, after Separation

Under SEM observation, the interfaces of samples processed under all three test conditions were similar. Figure 13 shows the interface of the specimen hot-pressed at 1200°C and Figure 14 is the interface picture of the one from 1500°C process. It was found that small grains were all over the interfaces in both pictures. The EDX investigation of two area ('A' and 'B') in Figure 14 shows that region 'A' is the barrier film and region 'B' is the TZM substrate. The EDX results from region 'A' and 'B' are shown in Figure 15 and 16, respectively.

Since the electron-specimen interactive volume in EDX is in the micron range, (and so was the thickness of the oxide film), elements' signal(s) from the TZM substrate might appear when the barrier film was investigated by EDX. This might explain the presence of small Mo signal in 'A' area, as shown in Figure 15. Therefore, the EDX results were not sufficient to claim that there was no inter-diffusion between the substrate and the barrier film. A more surface sensitive method, the AES line scanning, was used to verify the inter-diffusion behavior.

The interface of the specimen hot-pressed at 1300°C was examined by AES line scanning. The scanning line included both the substrate and film. Figure 17 shows the elemental signals of Al, O, and Mo along this line, with an arbitrary peak height unit. These signals also superimposed onto a SEM photograph in Figure 18. It was found that there was no

inter-diffusion between Mo and Al across the interface. The presence of oxygen signal on the substrate surface suggested that the substrate was oxidized on the interface of the TZM side. Because the bonding test was done under a high vacuum condition ( $10^{-5}$  to  $10^{-6}$  torr range) and  $\text{Al}_2\text{O}_3$  is a very stable material, the cause of the oxidation was presumed to be the excess oxygen in the as-deposited aluminum oxide film.

Thus, it is concluded that the TZM plates at high temperatures can be prevented from diffusion bonding by using the as-deposited aluminum oxide films. It is necessary to control the composition in the film to prevent oxidation of the TZM on its interface with the film. This control can be done by reducing the oxygen flow into the deposition chamber, because the oxygen content in the film now is in excess of the stoichiometry at present maximum oxygen flow.

#### 4. Summary

Aluminum oxide films deposited onto planar substrates (glass, TZM and brass), by a reactive d.c. sputtering method, were dense and had a higher O-to-Al ratio than the stoichiometric oxide. Thick films (of about  $2.42\text{ }\mu\text{m}$ ) on the TZM substrates successfully prevented diffusion bonding between the substrates up to  $1500^\circ\text{C}/10\text{ MPa}/6\text{ hours}$ . However, the TZM substrate was oxidized by the excess oxygen content of the film.



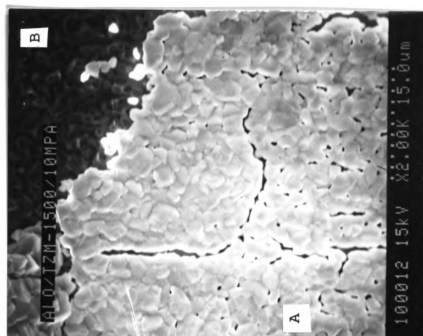


Figure 14. Interface of TzM Plate, after Hot-pressing at 1500°C, by SEM



Figure 13. Interface of TzM Plate, after Hot-Pressing at 1200°C, by SEM

X-ray: 0 - 20 KeV  
Live: 100s Preset: 100 s Remaining: 0s  
Real: 114s 12% Dead

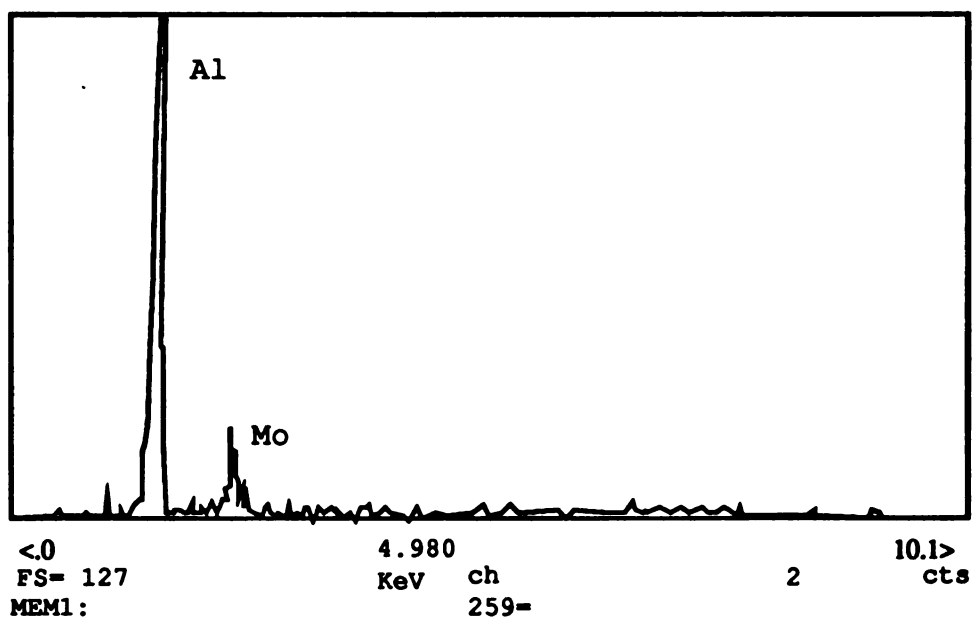


Figure 15. Region A of Figure 14, Surface Element Information, by EDX.

X-ray: 0 - 20 KeV  
Live: 100s Preset: 100 s Remaining: 0s  
Real: 114s 12% Dead

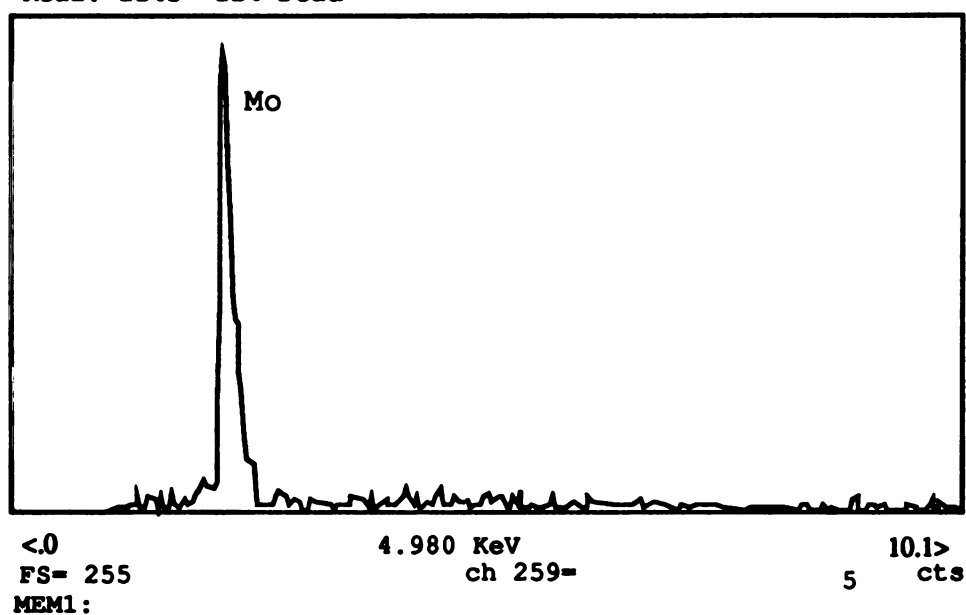


Figure 16. Region B of Figure 14, Surface Element Information, by EDX.

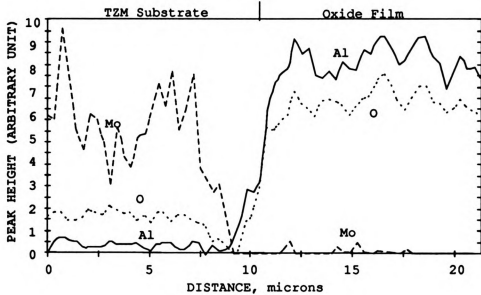


Figure 17. Line Scanning for Al, O, Mo, on the 1300 °C TZM Specimen, by AES

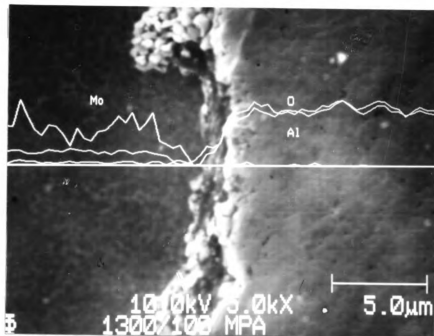


Figure 18. SEM of Line Scanning on the 1300 °C TZM Specimen, by AES.

## CHAPTER IV. AN $\text{Al}_2\text{O}_3$ DIFFUSION BARRIER FOR A $\text{SiC}/\text{Ni}_3\text{Al}+\text{B}$ COMPOSITE

### 1. Introduction

In the previous sections, the performance of thick sputter-deposited aluminum oxide films on planar substrates was discussed. These films performed successfully as diffusion barriers for preventing diffusion bonding between TZM plates up to 1500 °C for 6 hours, with a bonding pressure of 10 MPa. In the following sections, the fabrication and performance of thinner aluminum oxide films on SiC particulate substrates will be discussed. The particulates were incorporated into an intermetallic matrix composite with boron doped  $\text{Ni}_3\text{Al}$  as the matrix alloy. The goal of this study was to prevent the deleterious diffusion-controlled interface reactions in  $\text{SiC}/\text{Ni}_3\text{Al}+\text{B}$  system.

SiC particulate reinforcement of a  $\text{Ni}_3\text{Al}+\text{B}$  matrix may improve the creep resistance of the matrix at high temperature. This is important because  $\text{Ni}_3\text{Al}+\text{B}$  alloy itself suffers the loss of its yield stress and creep resistance with increasing temperature above 730 °C [Liu, 1985]. However, severe inter-diffusion and interfacial reaction between SiC and the  $\text{Ni}_3\text{Al}+\text{B}$  matrix causes degradation of the SiC particulate reinforcement and the formation of brittle

reaction products in interfacial region [Nieh, 1988; Yang (2) and Yang (3), 1989]. A barrier for preventing the diffusion-controlled reaction is therefore needed in this system. It was shown in Chapter II that  $\text{Al}_2\text{O}_3$  is a good diffusion/reaction barrier in  $\text{SiC}/\text{Ni}_3\text{Al}+\text{B}$  system. A  $0.13\text{ }\mu\text{m}$  thick  $\text{Al}_2\text{O}_3$  film formed by preoxidizing  $\text{Ni}_3\text{Al}+\text{B}$  alloy (IC-50) successfully prevented the diffusion bonding between the aluminide plate and a SiC disc up to  $1100\text{ }^\circ\text{C}$  [Nieh, 1988].

In this study, a different approach of film fabrication was employed. The aluminum oxide film was formed by the reactive d.c. sputtering technique. The effectiveness of the as-deposited film as a diffusion barrier was investigated in a SiC particulate reinforced  $\text{Ni}_3\text{Al}+\text{B}$  composite. A special levitation device was made to enable the deposition of the film onto the SiC particulates [Hillegas, 1990]. The film thickness used in this study was similar to that in Nieh's work. A diffusion bonding experiment was applied to obtain the SiC particulates/ $\text{Ni}_3\text{Al}+\text{B}$  composite for the oxide film performance study. In this study, the matrix was IC-15  $\text{Ni}_3\text{Al}+\text{B}$  alloy (Ni-24.76 at% Al-0.24 at% B).

## 2. Experimental Procedures

### 2.1. Al<sub>2</sub>O<sub>3</sub> Film Deposition and Examination

For film deposition, the sputtering source and conditions were the same as the film deposition onto planar substrates, as discussed in Chapter III, Section 2. The substrate here was a 240 grit abrasive SiC particulate with an average particle diameter of 60  $\mu\text{m}$ . In order to deposit film onto the surface of the particulates, a levitation device was made which consisted a signal generator, an amplifier, a speaker as vibrator, and a container for the particulates. The speaker and container were placed 8 inches below the sputtering target in the vacuum chamber. During the coating experiment, the amount of SiC powder was about 0.8 grams. The input to the 8  $\Omega$  speaker was a sine wave of 2 to 3 volts (peak-to-peak), i.e., about 0.25 to 0.6 Watts power for the speaker. After coating the particulate substrates, the films were examined by AES profiling to estimate the film thickness and by SEM to examine the film surface morphology.

### 2.2. Diffusion Bonding of SiC/Ni<sub>3</sub>Al+B Composites

The SiC particulates with the coated films were dispersed and sandwiched between two Ni<sub>3</sub>Al+B plates and then compressed in the MTS-810 as shown in Figure 19. The

diffusion bonding experiments were performed in vacuum at pressures of  $10^{-5}$  to  $10^{-6}$  torr, and the bonding conditions were:  $1000^{\circ}\text{C}/40\text{MPa}/1$  hour;  $1100^{\circ}\text{C}/40\text{MPa}/3$  hours; and  $1100^{\circ}\text{C}/40\text{MPa}/12$  hours. The specimen for the  $1100^{\circ}\text{C}/40\text{MPa}/12$  hours process was arranged in such a way that the SiC particulates on the half side of the specimen were uncoated while on the other side the SiC particulates were coated, as shown in Figure 19(b). Diffusion bonding was expected between two  $\text{Ni}_3\text{Al}+\text{B}$  plates after tests. After the bonding tests, the cross-section of the bonded couples was studied for the oxide film performance in the interfacial region by optical microscopy and AES.

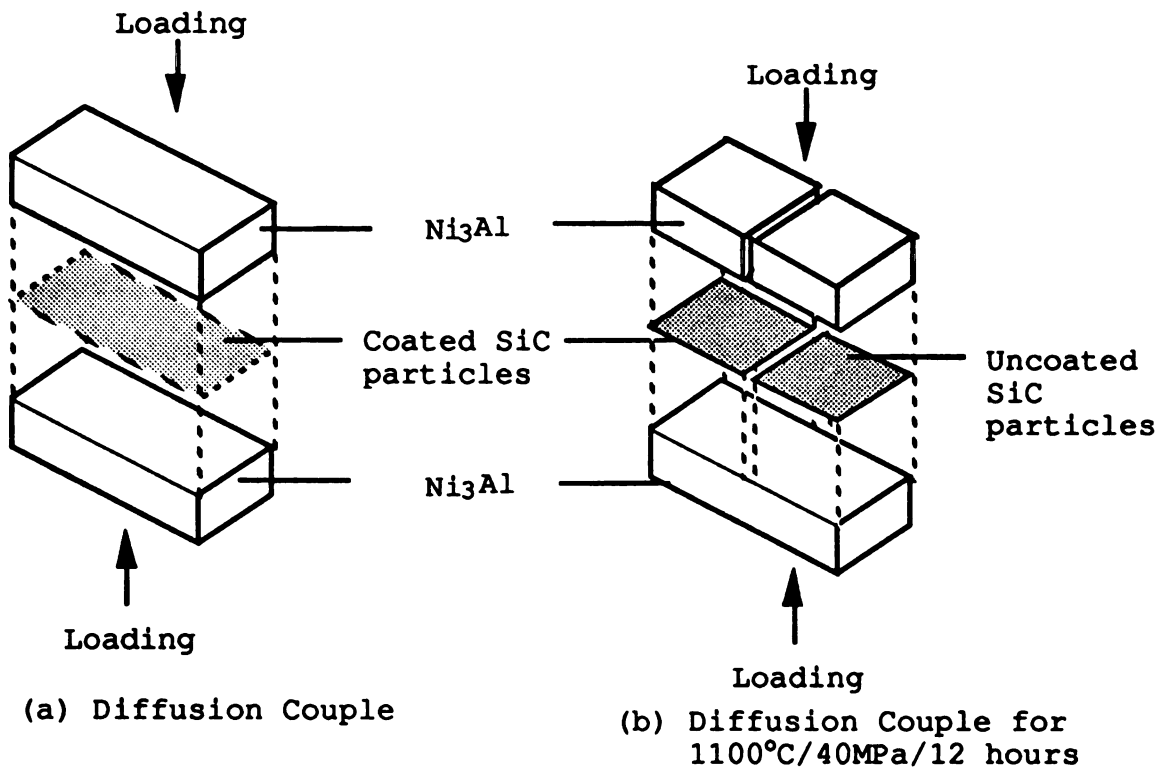


Figure 19: Configuration of SiC Particulates/ $\text{Ni}_3\text{Al}$  Diffusion Bonding Couple

### 3. Results and Discussion

#### 3.1. Film Deposition and Examination

During film deposition in a vacuum, it was observed that the SiC particulates were levitated in the container of the levitation device. The action of the levitator caused all particles to be exposed to the coating flux. The projected area of the coating flux was about 10 cm<sup>2</sup>. The planar deposition rate was measured during the deposition as if the substrate were plate. The rate was 300 Å/min..

Because the particulates had a much higher surface-to-volume ratio than the plate or bulk material, a much lower effective deposition rate, the film growth rate on the particulate substrate, is expected comparing to the planar deposition rate. Also, different *angle-of-incidence* at different locations on a particulate surface causes the deposition rate varying from point to point on the particulate. To simplify the discussion, the principle of Mass Conservation will be used next to discuss briefly the relationship between these two deposition rates.

During deposition, the projected area ( $A$ ) is about 10 cm<sup>2</sup>. Thus, the volume of depositing material within a period of time ( $t$ ) is:

$$V_1 = AR_0t$$

where  $R_0$  is the planar deposition rate for planar substrate under same condition. Assuming that the particulates are



spherical and the film thicknesses are identical on all the particulates, thus, the total volume of coated material on the particulates, after the same time  $t$ , can be expressed as:

$$V_2 = N\left(\frac{\pi}{6}\right)[(d + 2R_p t)^3 - d^3]$$

where,  $N$  is the number of particulates used in an experiment,  $d$  is the average diameter of the SiC particulates,  $R_p$  is the effective deposition rate for the particulate substrates, and  $R_p t$  represents the film thickness on the particulates.  $N$  can be expressed as:  $N = \frac{6W_p}{\rho\pi d^3}$ , here  $\rho$  is the density of the SiC particulates, and  $W_p$  is the weight of SiC particulates used in a deposition experiment. Since these two volumes are equal according to Mass Conservation principle, the relationship between two deposition rates ( $R_o$  and  $R_p$ ) then is:

$$\left(\frac{W_p}{\rho}\right)\left[\left(1 + \frac{2R_p t}{d}\right)^3 - 1\right] = AR_o t$$

In this experiment,  $\rho$ ,  $d$ ,  $A$ ,  $W_p$ ,  $t$  were 3.22 g/cm<sup>3</sup>, 60  $\mu$ m, 10 cm<sup>2</sup>, 0.8 g, and 2 hours, respectively. The effective deposition rate ( $R_p$ ) should be 12 Å/min. as calculated for a planar deposition rate ( $R_o$ ) 300 Å/min..

By AES profiling, the as-deposited film was found to be about 0.17  $\mu$ m thick after 2 hours deposition. The effective deposition rate onto the particulate substrate was 14 Å/min., which is close to the calculated one (12 Å/min.). The AES profiling curve for the as-deposited film is shown in Figure 20. On the figure, the O-to-Al ratio in this film was

similar to those in the films on the brass plates shown in Figure 8 and Figure 9. Therefore, it was presumed that the as-deposited films on SiC particulates had similar composition to those on the planar substrates.

Therefore, even though the effective deposition rate for the particulate substrate is lower than that for the planar one, there is no fundamental difference in reactive sputter deposition onto planar and particulate substrates.

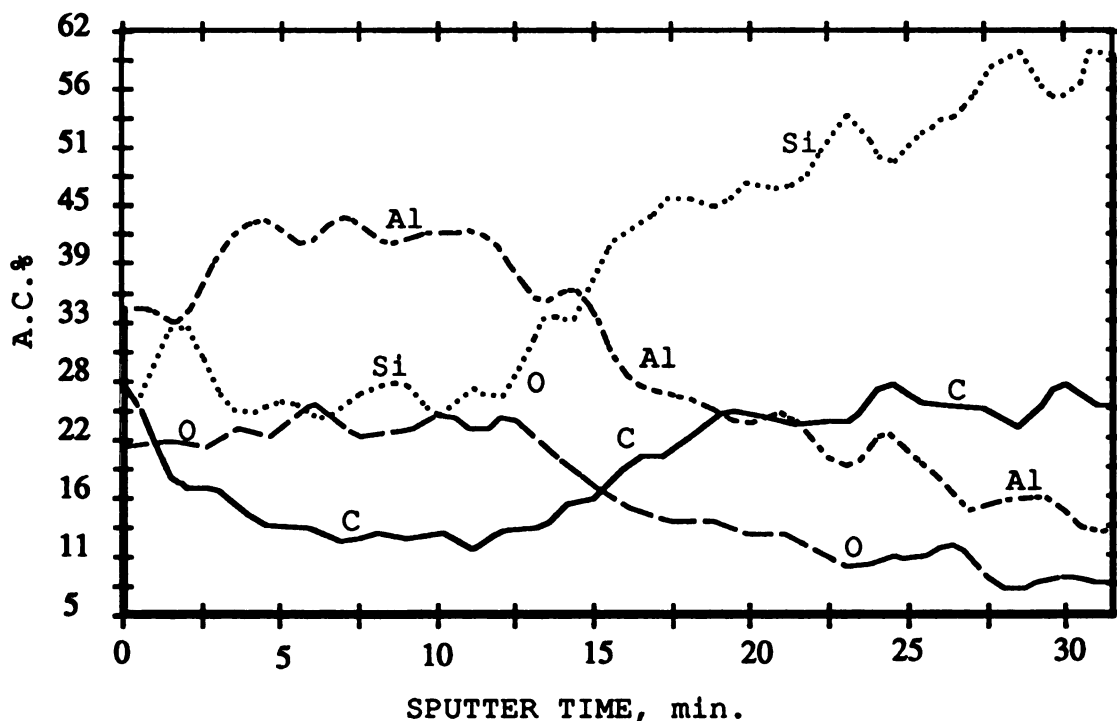


Figure 20. AES Profiling of Film on SiC Particulate

In the surface morphology study, the films on the most of the SiC particulates appeared dense and fully covered the particulates. However, the coating quality on some particulates appeared not as good as others, especially there is a sharp edge on the particulates. Figure 21 shows a region of discontinuous film at a sharp edge of a particulate. Individual columns separated by voids can be seen at that region. The film tends to be dense and void-free away from the edge. These defects may influence the performance of the films as diffusion barriers for the SiC/Ni<sub>3</sub>Al+B system.

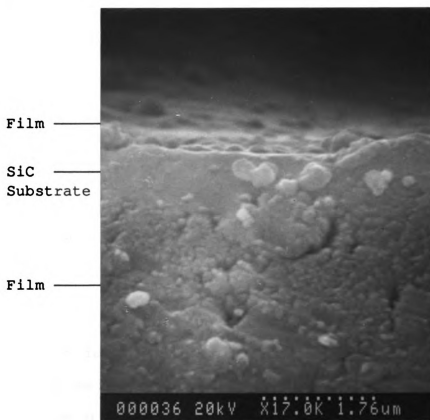


Figure 21. As-deposited Film on the Edge of a SiC Particulate Substrate, by SEM

### 3.2. As-deposited Oxide Films as a Diffusion Barrier for SiC/Ni<sub>3</sub>Al+B Composite

After the SiC/Ni<sub>3</sub>Al+B composite had been made, it was found that sufficient bonding of the Ni<sub>3</sub>Al plates did not take place under all conditions (up to 1100°C/40MPa/12 hours), and voids were often seen between two matrix plates. This was consistent with the findings of Lee [1990] that true metallurgical bonding of the matrix plates (IC-15, with a melting point 1387 °C) requires processing temperature of at least 1280 °C (for 2 hours at 20 MPa).

It was found that there was interaction between SiC particulates and Ni<sub>3</sub>Al plates even under these bonding conditions after polishing the samples to reveal their cross-sections. Figure 22(a) and 22(b) show the reaction region of the sample bonded at 1000°C: here Figure 22(a) is a micrograph for the as-polished sample and Figure 22(b) is a picture for the same sample after etched in 5g Na<sub>2</sub>SO<sub>4</sub> + 20ml HCl + 20ml H<sub>2</sub>O. This band structure of the reaction products is similar to those found by others [Nieh, 1988; Yang (2), 1989].

The specimen for the 1100 °C/40 MPa/12 hours process was arranged in such a way that the SiC particulates on the half side of the specimen were uncoated while on the other side the SiC particulates were coated. It was found that the uncoated SiC particulates totally disappeared, while the coated ones still had the remnant and reaction product layers

like those in the other specimens. Figure 23 shows both sides of this specimen. In the picture, the left side of specimen used the uncoated and right side used the coated SiC particulates. The result from this specimen shows clearly that the aluminum oxide film coatings have reduced the rate of the diffusion-controlled reaction between SiC and the matrix, even though it does not function well as a diffusion barrier in this composite system.

Thus, the sputter-deposited films on the SiC particulates did not function well as diffusion barriers for this composite. The film might be too thin to prevent the diffusion of Ni into the SiC particulates under the bonding conditions. The defects in the films, such as void and discontinuity, can cause direct contact between the matrix and the particulates. The thermal expansion coefficients mismatch among the SiC, the film and the matrix (mainly the  $\text{Ni}_3\text{Al}$ ) may also cause cracks in the films.

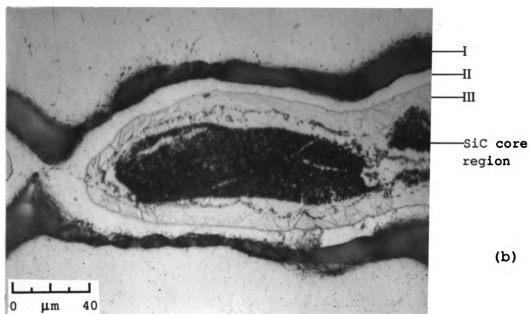
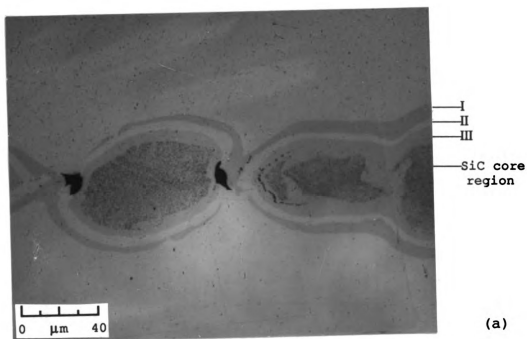
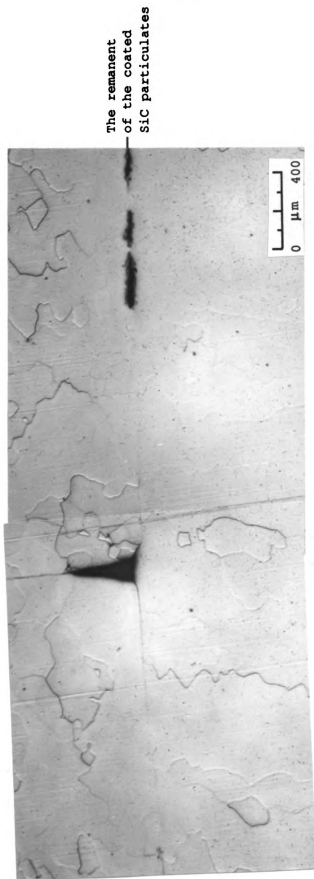


Figure 22. Optical Micrograph for Sample of 1000°C,  
500x: (a) As-polished; (b), Etched



Left Side: with Uncoated SiC  
Particulates

Right Side: with Coated SiC  
Particulates

Figure 23: Optical Micrograph for the Sample of 1100 °C/12 hours, 50x.

The elemental information across the reaction zone of the specimen from the 1100°C/40MPa/3 hours process was studied by AES line scanning. The results of four elements (O, Si, Ni and Al) detected along a line across the reaction zone are shown in Figure 24. This investigation was only qualitative and the peak height unit of these four signals were arbitrary in Figure 24. Figure 25 is a SEM picture superimposed by the line scanning results of Ni, Al, and Si signals.

The first (I) layer of the reaction zone (the outer layer) was the original place of the aluminum oxide film. Ni had penetrated the film into the SiC particulate. The abrupt changes of the Ni, Al, and O signals in this layer suggested the presence of a Ni-Al-O compound.

Ni signal in the second (II) layer was almost as strong as it is in the matrix, while the Al signal decreased. There was also some weak Si signals in this region. Therefore, in the second (II) layer, there were Ni-Al and/or Ni-Al-Si compounds.

In the third (III) layer, the Ni signal remained as strong as that in the second layer and the Si signal became stronger. The Al signal was almost down to the noise level in this layer. Therefore, the third layer appears to be an Ni-Si compound.



In the SiC core region, the same tendencies of Si and Ni signals suggested that nickel silicide(s) existed in this region. It has been found by others that in the SiC core region the phases were  $\text{Ni}_2\text{Si}$  and graphite [Yang (2), 1989].

The results from the AES study were similar to those of Nieh [1988] and Lee [1990]. Ni was the predominant diffusing species for this diffusion-controlled process. It diffused extensively into the SiC center region and formed many compound with Si, Al.

#### 4. Summary

By a special levitation device, aluminum oxide films can successfully be deposited onto SiC particulate substrates by reactive d.c. sputtering method. The films were presumed similar in composition to those on planar substrates. Owing to high surface-to-volume ratio, the effective deposition rate was very low.

The 0.17  $\mu\text{m}$  thick as-deposited aluminum oxide film did not stop diffusion-controlled reactions between SiC particulates and the  $\text{Ni}_3\text{Al}+\text{B}$  matrix. Ni diffused into SiC and Ni-Al-O compounds were formed between the matrix and the reaction region. Nevertheless, the oxide film on SiC particulates did delay the diffusion.

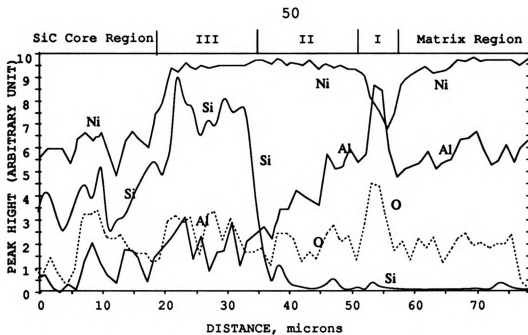


Figure 24. Line Scanning for Ni, Al, O, Si on the Sample of 1100 °C/3 hours, by AES.

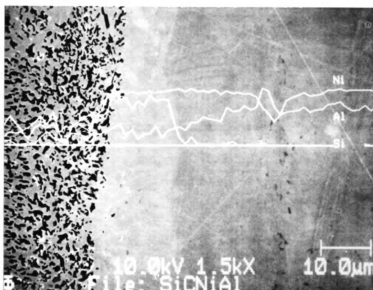


Figure 25. SEM Image of Line Scanning on the Sample of 1100 °C/3 hours, by AES.

## CHAPTER V. CONCLUSIONS

This research has employed aluminum oxide films, deposited onto both planar and particulate substrates by a reactive d.c. sputter deposition method, to act as diffusion barriers at high temperature. The films, if sufficiently thick, can be used as effective diffusion barriers for very high temperature applications. With oxygen added to the working gas, the d.c. magnetron sputtering of aluminum forms dense aluminum oxide films on the planar substrates. On the particulate substrates, however, the coating quality of the films were not as good as those on the planar substrates.

The as-deposited aluminum oxide film by the reactive d.c. sputter deposition had a higher O-to-Al ratio than stoichiometry. This ratio was between 1.97 to 2.12, indicating that the film composition is  $\text{Al}_2\text{O}_x$ , where  $x$  is between 3.94 and 4.24. This composition was found throughout the films on both planar and particulate substrates.

The as-deposited film was an excellent diffusion barrier for TZM alloy. With 2 layers of 2.42  $\mu\text{m}$  thick films between two TZM plates, no bonding between these TZM plates was achieved up to 1500 °C for 6 hours with a loading pressure of 10 MPa. While no inter-diffusion resulted among the TZM substrate elements and Al in the film, the interface on the

substrate side was oxidized due to the excess oxygen in the film.

When applied as a diffusion/reaction barrier for SiC particulates reinforced Ni<sub>3</sub>Al+B alloy (IC-15) composite, the as-deposited film with a thickness of 0.17  $\mu\text{m}$  did not prevent elemental diffusion between the SiC particulates and Ni<sub>3</sub>Al+B matrix. Ni in the matrix was the predominant diffusing species in the system while the inter-diffusion of Al and Si was limited. Banded structures were seen in the reaction zone. Many Ni-Al, Ni-Si, and Ni-Al-Si compounds were apparently formed in these structures. A Ni-Al-O compound existed on the boundary of the reaction zone. Nevertheless, the film did reduce the rate of diffusion-controlled reaction in SiC/Ni<sub>3</sub>Al+B composite.

The thickness of the Al<sub>2</sub>O<sub>3</sub> film on SiC particulates, which was 0.17  $\mu\text{m}$ , was found inadequate to act as a diffusion barrier for SiC particulate/Ni<sub>3</sub>Al+B composite. Voids in the films could cause direct contact between the matrix and the particulates. The thermal expansion coefficients mismatch among SiC particulates, the aluminum oxide films, and the Ni<sub>3</sub>Al+B matrix could cause the films to break. Also, the unevenly distributed stress field on the SiC particulates and the films during the bonding processes might play a role in this failure. More work needs to be done in order to use such reactive d.c. sputter-deposited aluminum oxide films as good diffusion/reaction barriers for the SiC/Ni<sub>3</sub>Al+B system.

Future research may include controlling the composition of the oxide film. Ion beam assisted deposition may also be necessary to improve the coating quality. With a low-energy secondary beam bombarding the growing film, the as-deposited film will have a better adherent quality and tend to be fully dense. Also, the HIP process, in which the SiC particulates and matrix material powders are hydrostatically hot-pressed to form a dense composite, may be useful. In such processes, an evenly distributed compressive stress around the particulates may help the barrier films function.

## **BIBLIOGRAPHY**

- Behrisch, R., Ed., Sputtering by Particle Bombardment I, Springer-Verlag, 1981.
- Behrisch, R., Ed., Sputtering by Particle Bombardment II, Springer-Verlag, 1983.
- Brindley, P. K., "SiC Reinforced Aluminide Composites", High-Temperature Ordered Intermetallic Alloys. II, pp. 419-424, 1987.
- Broutman, L. J. and Krock, R. H., Composite Materials Voll: Interfaces in Metal Matrix Composites, Ed. by Metcalfe, A. G., Academic Press, 1974.
- Brown, L. D., Maruyama, B., Cheong, Y., Rabenberg, L., and Marcus, H. L., "Metal Matrix Interfaces and their Impact on Mechanical Behavior of Composites" Composite Interface, Ishida, H. and Koenig, J. L., Ed. Elsevier, 1986.
- Chou, T. W., Kelly, A. and Okura, A., "Fibre-Reinforced Metal-Matrix Composites", Composites, 16, pp. 187-206, 1985.
- Goshtagore, R. N., J. Appl. Phys., 40, pp. 4374, 1969.
- Grayson, M., Ed., Encyclopedia of Composite Materials and Components, 1983.
- Hall, E. L., Kouh, Y. M., Jackson, M. R., and Mehan, R. L., "Chemistry and Distribution of Phase Produced by Solid State SiC/NiCrAl Reaction", Metall. Trans A., 14A, pp. 781-790, 1983.
- Hillegas, D.S., Private Communication, SoloHill Eng., Ann Arbor, Michigan, 1990.
- Holland, L., "The Basic Principles of Sputter Deposition", Science and Technology of Surface Coating, Ed. by Chapman, B. N., Academic Press, 1974.
- Jackson, M. R., Mehan, R. L., Davis, A.M., and Hall, E. L., "Solid State SiC/Ni Alloy Reaction", Metall. Trans A., 14A, pp. 355-364, 1983.
- Kendall, E. G., "Development of Metal-Matrix Composites Reinforced with High-Modulus Graphite Fibres", Composite Materials, Vol. 4: Metallic Matrix Composites, Ed. by Kreider, K. G., pp. 319-397, 1974.

- Lee, C., Grummon, D., and Gottstein, G., "Microstructure and Interface Behavior in Diffusion Bonded Ni<sub>3</sub>Al Matrices Containing Continuous Al<sub>2</sub>O<sub>3</sub> Fibers", in Intermetallic Matrix Composites, MRS, Vol. 194, 1990.
- Liu, C. T. and White, C. L., "Design of Ductile Polycrystalline Ni<sub>3</sub>Al Alloys", Intermetallic Compound L, 39, pp. 360-380, 1985.
- Mattox, D., Materials Research Society Short Course on Films and Coating Deposition Techniques, 1989.
- Mehan, R. L. and Bolon, R. B., "Interaction between Silicon Carbide and a Nickel-based Superalloy at Elevated Temperatures", Journal of Materials Science, 14, pp. 2471-2481, 1979.
- Mehan, R. L. and Noone, M. N., "Nickel Alloys Reinforced with  $\alpha$ -Al<sub>2</sub>O<sub>3</sub> Filaments", Composite Materials, Vol. 4: Metallic Matrix Composites, Ed. by Kreider, K. G., pp. 159-227, 1974.
- Metcalfe, A. G., "Fiber-Reinforced Titanium Alloys", Composite Materials, Vol. 4: Metallic Matrix Composites, Ed. by Kreider, K. G., pp. 269-318, 1974.
- Nieh, T. G., Stephens, J. J., Wadsworth, J., and Liu, C. T., "Chemical Compatibility between Silicon Carbide and a Nickel Aluminide", High-Temperature Ordered Intermetallic Alloys. III, pp. 215-224, 1989.
- Nourbakhsh, S., Margolin, H., and Liang, F. L., "Microstructural Observations of Pressure Cast Ni<sub>3</sub>Al/Al<sub>2</sub>O<sub>3</sub> and Ni/Al<sub>2</sub>O<sub>3</sub> Composites", Metall. Trans. A, 20A, pp. 2159-2166, 1989.
- Pang, T. M., Scherer, M., Heinz, B., Williams, C., and Chaput, G. N., "A Modified Technique for the Production of Al<sub>2</sub>O<sub>3</sub> by Direct Current Reactive Magnetron Sputtering", J. Vac. Sci. Technol., A7, pp. 1254-1258, 1989.
- Pope, D. P., "High Temperature Ordered Intermetallic Alloys", High-Temperature Ordered Intermetallic Alloys II, pp. 3-11, 1987.
- Reddy, S. N. S., Betrabet, H. S., Purushothaman, S. P., and Narayan, C., "Interface Mixing between Metals and Ceramics: Classification, Thermochemistry, and Processing", Ceram. Eng. Sci. Proc., 10(11-12), pp. 1696-1707, 1989.



- Savitskii, E. M. and Burkhanov, G. S., Physical Metallurgy of Refractory Metals and Alloys, Consultants Bureau, 1970.
- Schoutens, J. E. and Tempo, K., Introduction to Metal Matrix Composite Materials, DOD MMCIAC #272, June 1982.
- Shewmon, P. G., Diffusion in Solids, McGraw-Hill, 1963.
- Verhoeven, J. D., Fundamentals of Physical Metallurgy, Wiley & Sons, 1975.
- Walters, R. P. and Covino, B. S., Jr., "Evaluation of High-Temperature Diffusion Barriers for the Pt-Mo System", Metall. Trans. A, 19A, pp. 2163-2170, 1988.
- Westwood, W. D., "Sputtering Deposition Processes", MRS Bulletin, pp. 46-51, Dec. 1988.
- Yang, J.-M., Kao, W. H., and Liu, C. T.(1), "Development of Nickel Aluminide Matrix Composites", Materials Science and Engineering, A107, pp. 81, 1989.
- Yang, J.-M., Kao, W. H., and Liu, C. T., (2), "Interface Characterization of Fiber-Reinforced Ni<sub>3</sub>Al Matrix Composites", Metall. Trans. A, Vol. 20A, pp. 2459-2469, 1989.
- Yang, J.-M., Kao, W. H., and Liu, C. T., (3), "Reinforcement/Matrix Interaction in SiC Fiber-Reinforced Ni<sub>3</sub>Al Matrix Composites", High-Temperature Ordered Intermetallic Alloys. III, pp. 453-458, 1989.

MICHIGAN STATE UNIV. LIBRARIES



31293008825683